

Enhanced earthquake risk of Kingston due to wave field excitation in the Liguanea Basin, Jamaica

MARGARET D. WIGGINS-GRANDISON^{1,2}, TAREK R. M. KEBEASY^{1,3}
AND EYSTEIN S. HUSEBYE¹

¹*Institute of Solid Earth Physics, University of Bergen, 41 Allégaton, Bergen 5007, Norway.*

²*Earthquake Unit, University of the West Indies-Mona, Kingston 7, Jamaica.*

³*National Research Institute of Astronomy and Geophysics, Cairo, Egypt.*

ABSTRACT. Kingston, the capital of Jamaica, an island in the Northern Caribbean, is situated on the Liguanea alluvial plain. Based on intensity reports over several hundred years, the alluvial plain is generally associated with an enhanced level of earthquake risk in Kingston. Two recently acquired 2-D depth profiles across the plain have made it possible to model the 2-D wave-field response of the Liguanea basin. Finite difference modeling was used to investigate the effect of the basin and surrounding topography on local shear-wave sources emanating from north, south and east of the basin. The results show that energy partitioning across layer boundaries, location within the basin, and source position in general, determined the level of wave-field amplification within the sediments. In the extreme, amplitudes were highest by one order of magnitude unit (a factor of 10) at the hill-basin margins and at the margins nearest to the sources. Amplitudes were slightly lower at the centre of the basin and away from the source, especially when the alluvium was thick. When high inelastic attenuation of the sediments and the upper 3 kilometres of crust were introduced, the amplitude of ground motion was reduced only marginally. The results predict variability on a scale of a few hundred metres for ground motion over the Liguanea Plain that cannot be neglected in future seismic risk studies. Additionally, it was determined that the characteristic frequency for the Liguanea alluvium is about 6 Hz.

1. INTRODUCTION

The Liguanea Plain is but one of the alluvial basins found along Jamaica's south coast. On this plain, the city of Kingston and the Port of Kingston are located. Kingston, the capital of Jamaica, has over 500,000 inhabitants, and is the commercial, economic and industrial centre of the country. Shepherd and Aspinall (1980) analyzed more than 300 years of historical records (Tomblin and Robson, 1977), and found that the city and villages on the Liguanea Plain experienced the highest rates of shaking in Jamaica with 20 instances of intensity VI and higher per century. This is equivalent to the rate experienced in the Los Angeles area, California for the last century (Shepherd and Aspinall, 1980). However, the island is located in a zone of moderate to low seismicity associated with the Caribbean plate along its northern boundary, where the tectonic environment is dominated by left-lateral east-west strike-slip deformation with north-south compression (DeMets *et al.*, 2000; Wiggins-Grandison, 2001; Van Dusen and Doser, 2000; Perrot *et al.*, 1997). It is thought that seismic waves from moderate to strong

earthquakes occurring near Jamaica are being amplified by sediments of presumably moderate thickness that make up the Liguanea Plain.

From the above we see that the relatively thin, topmost crustal layer of alluvium may significantly contribute to the earthquake hazard of Jamaica's major city, Kingston, and the Port of Kingston. Just how much, is the subject of this study. We start with a brief presentation of the geological setting of the area and give details on the seismicity. This information is needed for undertaking in a systematic manner, 2-D Finite-Difference wave-field simulation across the Liguanea Plain using realistic earthquake sources.

2. GEOLOGICAL SETTING AND SEISMICITY

The Oriente Fracture Zone (OFZ) skirting the southeastern coast of Cuba marks the boundary of the North American and Caribbean tectonic plates (Fig. 1). One of the most seismically active features in the Northern Caribbean, the overriding sense of movement along the OFZ is left-lateral strike slip (DeMets *et al.*, 2000; Van Dusen and Doser, 2000; Perrot *et al.*, 1997). Earthquakes with magnitude of

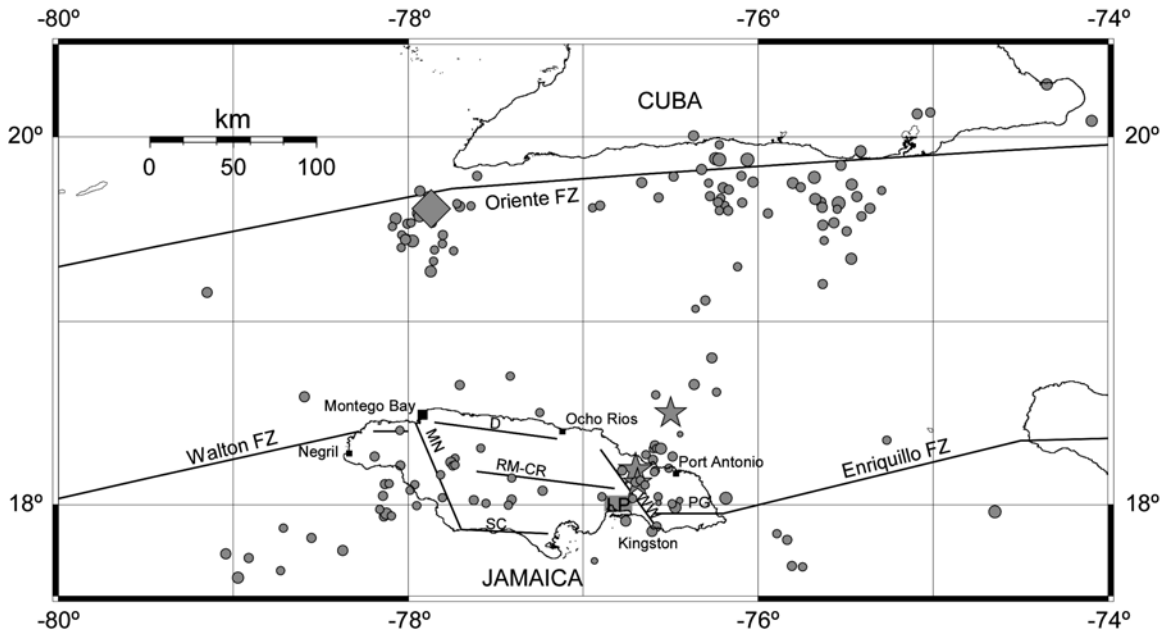


Figure 1. Geological setting and seismicity ($M \geq 3.0$) around the Liguanea Plain (LP); FZ = fracture/fault zone; major faults on Jamaica are MN = Montpelier-Newmarket, D = Duanvale, RM-CR = Rio Minho-Crawle River, SC = South Coast, WW = Wagwater, PG = Plantain Garden; diameters of epicentres are scaled to magnitude; diamond is the Cabo Cruz event with $M_w 6.9$; stars are epicentres of earthquakes that have caused damage on the Liguanea Plain in the 20th Century, from the north 1914, 1907, 1993 (see Table 1 for details).

the order of 7 occur on the OFZ in the vicinity of Cuba, roughly 200 km north of Kingston. In 1992, such an event at Cabo Cruz resulted in intensities of only IV on the Liguanea Plain (JSN bulletin,

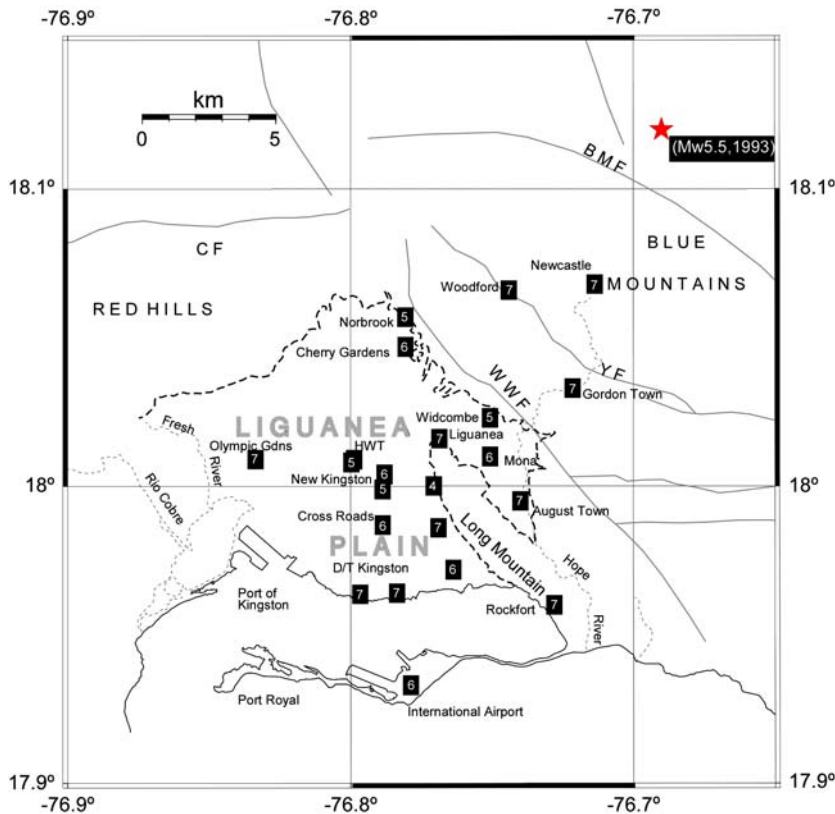


Figure 2. The Liguanea Plain (enclosed by heavy dashed line) and intensities due to the January 13, 1993, $M_w 5.5$ (HRV) earthquake; epicentre is marked with a star; CF = Cavaliers fault; BMF = Blue Mountains fault; YF = Yallahs fault; WWF = Wagwater fault.

Enhanced earthquake risk of Kingston

Table 1. Historic earthquakes (Tomlins and Robson, 1977; Wiggins-Grandison, 1996) that caused damage on the Liguanea Plain and are believed to have originated on eastern Jamaican faults. Epicentres for 20th Century events are shown in Figure 1

Date, time and epicentre (if known)	Maximum Intensity	Reported damage
March 1, 1688	VII	Houses and ships at Port Royal damaged
June 7, 1692 11:40 EST	X	2,000 of 8,000 inhabitants of Port Royal died, 75% of the buildings collapsed and/or sank into the sea due to liquefaction, a '6-foot' sea-wave crossed the harbor, houses in Liguanea and other south coast towns destroyed, water ejected from wells, large landslides in mountains of eastern Jamaica, some dammed rivers, aftershocks were felt daily up to September that year.
September 3, 1771	VII	Damage to structures, felt on boats at Port Royal.
January 14, 1907 15:29 EST 18.2°N 76.7°W	IX Estimated Ms 6.5	1,000 died, 90,000 homeless, buildings collapsed, in Kingston ensuing fires burned 56 acres, water mains broken, statues rotated, rail lines twisted and bent, spring at Rockfort increased flow, slumps around the harbor, landslides in the mountains, liquefaction at Port Royal caused 45 degree tilt in one building, international communication cables on the sea floor east of the harbor broken, tsunami on north coast.
August 3, 1914 6:25 EST 18.5°N 76.5°W	VII M 6.0	Buildings cracked in Kingston, door and window frames twisted, clocks stopped, stocks in drug stores broken.
January 13, 1993 12:11 EST 18.1°N 76.7°W	VII Mw 5.5 (HRV)	Everyone frightened and many rushed outdoors. Shaking lasted up to 12 seconds on the Liguanea Plain. Few cases of structural damage to buildings, e.g., damaged columns; mostly non-structural damage such as cracked walls and items being thrown off shelves, businesses closed to clean up, schools closed; increased flow at spring in Rockfort; many small landslides in the mountains blocked roads; some pipelines broken at joints; some unreinforced and under-reinforced buildings in very poor condition or on poor soils, collapsed; 2 broken unreinforced brick chimneys in the mountains [The Journal of the Geological Society of Jamaica 1996, 30: 60 pp]

1992). Note, the crust between Cuba and Jamaica is typical oceanic and, as such, is a poor propagation medium for damaging high frequency shear waves (Mendi *et al.*, 1997). Other faults associated with the wider plate margin, the Enriquillo Fault (EFZ) and the Walton Fault (WFZ) are not known to have produced earthquakes with damaging consequences on the Liguanea Plain.

The Liguanea Plain is a Quaternary alluvial fan of the Hope River that drains the mountains to the northeast of Kingston (Ahmad and Robinson, 1994) (Fig. 2). It consists of poorly sorted sands and gravels interspersed with layers of clay and sand. Occasionally, boulders of volcanic rock and conglomerate are also found (Ahmad and Robinson, 1994). The fan rises gently from sea level at Kingston Harbor to more than 200 metres elevation at Mona, in the northeast, where it meets the current Hope River at the base of the mountain range. It is bordered to the east by the NW trending Wagwater fault, which is associated with many micro-earthquakes. These micro-earthquakes, located in and around the Liguanea Plain, imply active faulting in the crystalline crust beneath the basin. Though small earthquakes dominate the local seismicity of Jamaica, larger events do occur,

particularly in the mountains above the Liguanea Plain.

On January 13, 1993, a moderate earthquake of magnitude Mw 5.5 (HRV) with focal depth around 15 km occurred, which caused intensities of VII in Kingston and neighboring areas (Wiggins-Grandison, 1996) (Fig. 2). Structural damage was observed in only a few larger multi-storey buildings, which are engineered structures (Adams, 1996). The damage to one and two-storey dwellings, that are typically non-engineered structures, ranged from minor to severe cracking (Adams, 1996; Harris, 1996). This varied with type and condition of the building and site conditions. For the Liguanea Plain, dwellings in Barbican (just north of Liguanea, Fig. 2) and August Town areas were mostly affected (Harris, 1996). It is now thought that Jamaica's historical damaging earthquakes may also have taken place on faults within 20 km of the Liguanea Plain due to the location of landslides in the nearby mountains and similar intensity patterns as the 1993 event (Wiggins-Grandison, 1996; National Disaster Research Inc *et al.*, 1999). These are listed in Table 1.

The Caribbean Uniform Building Code recommends for all Jamaica the use of SEAOC

Table 2. 1-D amplification factors in selected parts of the Liguanea Basin using SHAKE21 by NDR. *et al.* (1999)

Site, depth of alluvium/basement rock	Frequency (Hz)			
	0.5	1.0	10.0	30.0
1. Elleston Flats, basement rock at ~110 m	2.2	1.5	0.67	1.0
2. Buttercup Park, >200 m alluvium	0.9	0.7	1.7	1.1
3. National Heroes Circle, > 300 m alluvium	0.4	1.1	0.43	0.23

(Structural Engineers Association of California) seismic zone factor, $Z = 0.75$, which is equivalent to an acceleration of $0.3g$ on rock. Engineered structures generally conform to the code, whereas the level of compliance for non-engineered structures is not known (Adams, 1996). However, owing to the island being in the Caribbean hurricane belt, buildings are expected to withstand wind speeds of 200 km per hour. Since the last century, the majority of buildings in Kingston are of reinforced concrete, and are therefore strong enough to resist at least moderate earthquake forces, equivalent to say I – VII. The strength of the housing stock was evident in 1988, when a category IV hurricane hit the island. The overwhelming damage to reinforced structures was the loss of light roofs, which was attributed to complacency, as the island had experienced no hurricane in 51 years, and contractors had neglected to use hurricane straps to tie roofs to the structures.

3. PAST STUDIES

Shepherd and Aspinall (1980) used the SHAKE program to examine the extent of 1-D seismic wave amplification across the Liguanea Plain. In their model, the maximum thickness of the alluvium was 350 metres, and three earthquake sources of magnitudes 6, 7 and 7.5 were located at distances of 50 km, 80 km and 160 km, respectively. The results indicated a peak acceleration of $0.3g$.

Since the 1993 earthquake, it is acknowledged that faults closer than 50 km to Kingston are capable of generating earthquakes with moderate to high intensities (JSN bulletin, 1993; Wiggins-Grandison, 1996; NDR *et al.*, 1999). National Disaster Research *et al.* (1999) performed a seismic hazard assessment of Kingston, which incorporated local earthquake sources and a site response analysis for the Liguanea Plain, based on existing well logs. Few wells dug in the fan sediments have reached bedrock, hence the shape of the underlying basement and the thickness of the alluvium, are not well known. To rectify this lack of knowledge a gravity survey was conducted along two transects across the Liguanea Plain (Fig. 3a). The results revealed basement depths of about 60 m at the

northern limit, gradually deepening to 500-600 m at Kingston Waterfront. More uniform depths of 300-400 m with some undulations were found along an east-west profile (NDR *et al.*, 1999). The average shear-wave velocity of the fan sediments was estimated from well logs to be 320 – 500 m/s and the basement rock was assumed to be Miocene Limestone. Based on this new knowledge, bearing on alluvial thickness, phase velocities, well logs and local earthquake sources, SHAKE21 (Kagawa, 1995) was once more used to obtain 1-D peak ground accelerations at selected sites on the Plain and at four frequencies, 0.5, 1.0, 10 and 30 Hz. The seismic hazard results indicated peak accelerations in the range of $0.45g$ for the Liguanea Plain. The SHAKE results yielded amplifications up to a factor of 2 for selected sites (Table 2), but advise that the results should be viewed with extreme caution, as geotechnical information was estimated based on the well logs.

The opportunity of having 2-D profiles across the Liguanea Plain is herein exploited further by modeling the 2-D effects of the sedimentary basin on local shear-wave fields.

4. THE CRUSTAL MODEL

The basin was modeled along both the north-south and east-west gravity transects, which are, respectively about 10 km and 12 km long (Fig. 3a). The topography and depth to basement were replicated. Beyond the transects where the basin depth is unknown, the sediments were tapered at each end to merge with the crystalline free surface. The edges of the models were extended laterally to include the respective earthquake sources, as shown in Figure 3 and detailed in Table 3a. The sources, though restricted to the planes of the respective transects, are in positions typical of local seismicity. Below the basin, the model incorporates the P-wave crustal model for Jamaica, which consists of four layers over a half-space at 23 km (Wiggins-Grandison, in preparation). The source for each wave-field simulation was a shear wave source with a centre frequency of 2.5 Hz, which coincides with the peak amplitude commonly observed in the S-wave source spectra of many local earthquake recordings in Jamaica (Wiggins-Grandison and

Enhanced earthquake risk of Kingston

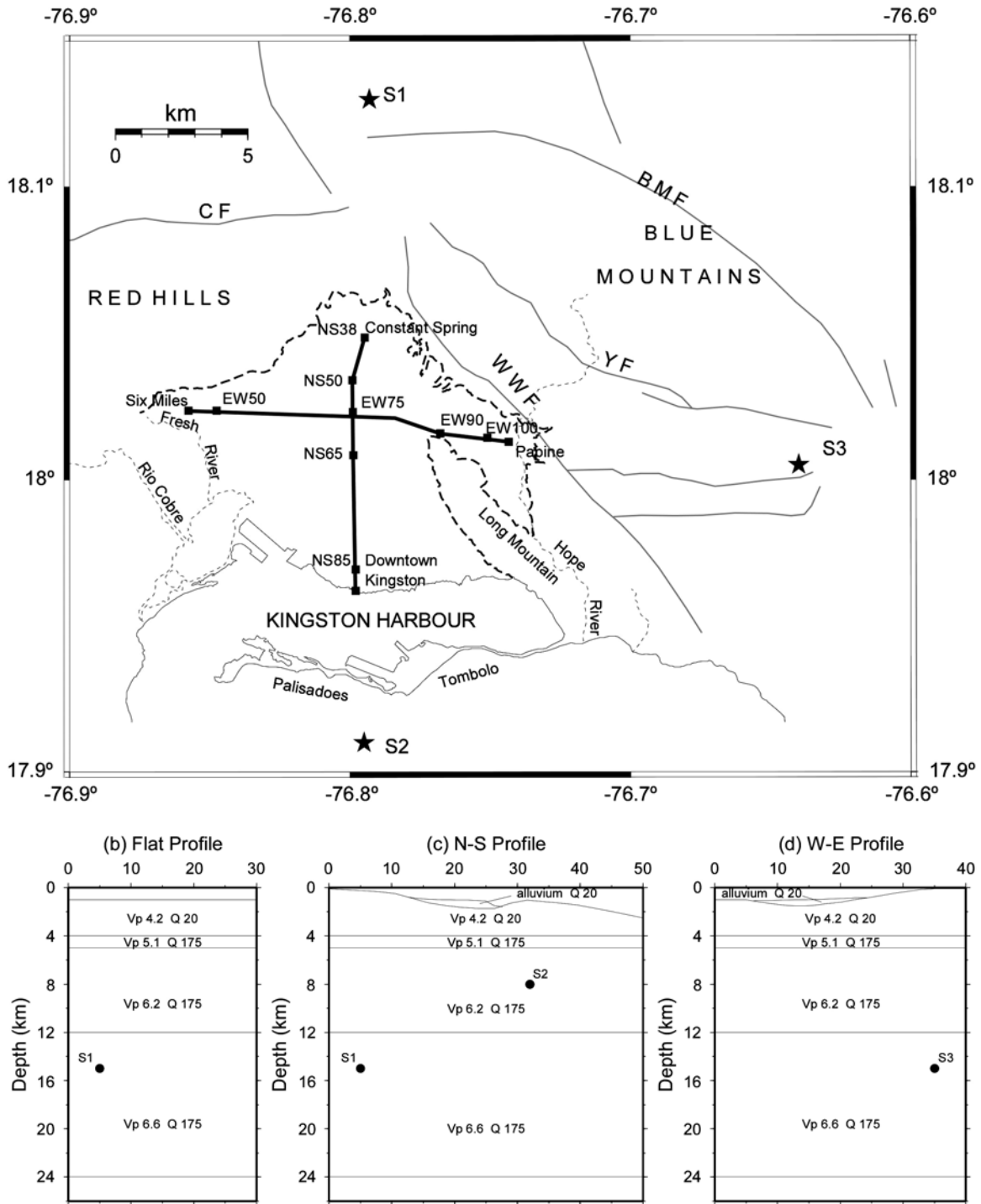


Figure 3. (a-upper) The two gravity transects (broad, grey lines): north-south transect from Constant Spring to Kingston Harbour, east-west from Papine to Six Miles, and, the positions of the three sources modelled S1, S2 and S3 (see Table 3); faults are as in Figure 2; numbers (e.g. NS50) indicate receiver positions for the seismograms used in Figure 6; (b) model A, flat layers = crustal model for Jamaica with source 1 and model D parameters; (c) depth profile of the N-S transect showing positions of sources 1 and 2; (d) depth profile of the W-E transect with source 3.

Table 3. (a) Sources used in the FD synthetics and relevant profiles; (b) Layer Q-values for each model - model B has the same Q throughout, model C has a low Q for the sediments only, whereas the control model, A, and model D have low Q applied to the upper 3 km, including the sediments in D.

Table 3a

Source	Profile	X (km)	Z (km) depth
1	North-south	5, from North	15
2	North-south	32, from North	8
3	West-east	35, from West	15

Table 3b

Model	Rock Q (> 3 km)	Near-surface Q (0-3 km)	Alluvium Q
A	175	20	flat layers, no basin
B	175	175	175
C	175	175	20
D	175	20	20

Havskov, in preparation) and elsewhere (Kebeasy and Husebye, 2003). The shear wave source was used, as S-waves are far more damaging than P-waves. A grid spacing of 10 m was used in order to provide good resolution and also in consideration of computing time constraints. A time step of 0.5 ms was computed from the established stability criterion for the finite-difference computations (Hestholm and Ruud, 2000). The vertical and horizontal particle velocity components of the synthetic wave field were computed at points spaced 200 m along the surface of the model.

Four models employing different Q configurations for the sediments and the uppermost crustal layer were used to investigate the relative influence of Q in the sediments and the uppermost crystalline part of the crust on the wave-field (Table 3b). For frequencies around 2.5 Hz, the average crustal Q was taken to be 175, whereas the value of Q for both the alluvium and the near-surface layer is 20 (Wiggins-Grandison and Havskov, in preparation). Shear-wave velocities were computed for rock layers from the P velocity using $V_p/V_s = 1.730$, which is the average determined for Jamaica (Wiggins-Grandison, in preparation). An average shear-wave velocity of 350 m/s was assumed for the alluvium in keeping with the range recommended by NDR *et al.* (1999), based on geologic analogues to the Liguanea Plain, and the 1997 NEHRP (National Earthquake Hazards Reduction Program Recommended Provisions) Site Classification D or ‘Stiff Soil’, which seems appropriate for these sediments.

The wave-field was synthesized using a 2-D finite-difference approach for viscoelastic media including surface topography, formulated by Hestholm and Ruud (2000) and Ruud and Hestholm (2001). The method was first applied to source 1 in model A, which has flat layers, with

near-surface attenuation in layer 1 (i.e., low Q in the upper 3 km), but no basin (Table 3, Fig. 3b). This served as the control model. In turn, the wave-field was synthesized for each of the sources 1 to 3 applied to models B, C and D, creating nine model-source combinations. These results were compared with that from the control-model.

5. RESULTS

The wavefronts propagating through the models were examined using snapshot displays. Three lapse times, of 4.7, 5.7 and 7.6 seconds, were selected to illustrate the wave-fields of the control model and the basin of model D for sources 1 to 3 (Fig. 4). Preliminary observations of the snapshots for models B, C and D for a given source revealed no significant differences, only small changes in the amplitudes, which are discussed later. This demonstrates that the velocity contrast between the crystalline rocks and the sediments is the major factor controlling the pattern of amplification in the basin. Model D is used to illustrate what happens in the basin, because it has the same Q distribution as the control model, and a near-surface Q-value of 20 making it a realistic model. Therefore, the only difference between models A and D is due to the presence of the basin and the topography that goes with it (i.e., the shape and thickness of the low-velocity sediments). Comparing these two models then, will satisfy the main aim of this study, that of examining wave-field excitation due to fan sediments in the Liguanea Basin.

The snapshots show the S-waves spreading outward and upward from the various sources (Fig. 4). Shear waves dominate but S-to-P conversions are clearly visible at layer interfaces. The refractions are strongest in the uppermost layer due

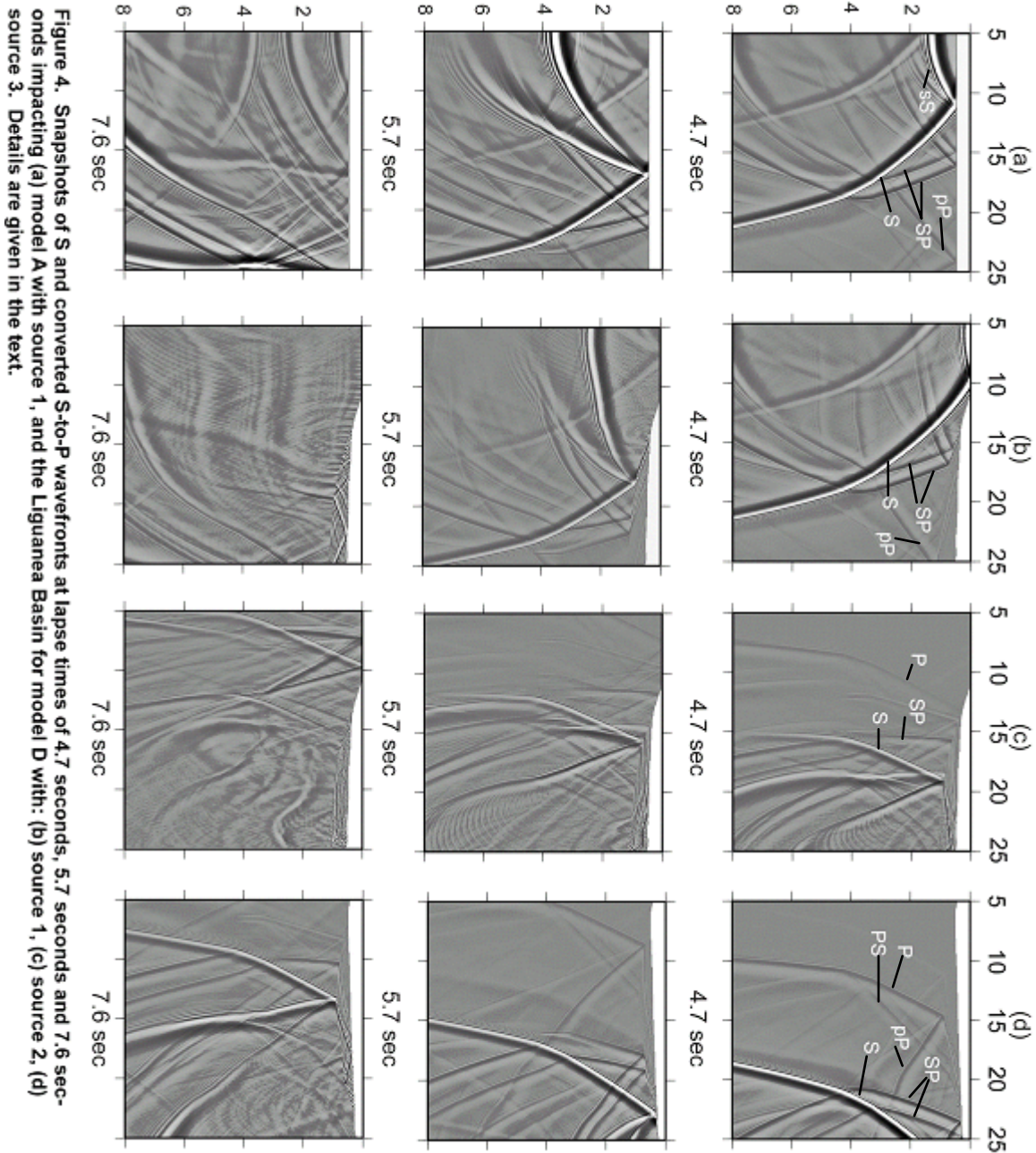


Figure 4. Snapshots of S and converted S-to-P wavefronts at lapse times of 4.7 seconds, 5.7 seconds and 7.6 seconds impacting (a) model A with source 1, and the Liguanea Basin for model D with: (b) source 1, (c) source 2, (d) source 3. Details are given in the text.

to the large velocity contrast between sediments and the crystalline rocks. Therefore, the angle of incidence is reduced at successive interfaces as the wave-field propagates upward through the model. The converted S-to-P-waves reach the surface before the main S-wave. These converted P-waves when reflected from the free surface, create a new set of down-going P- and S-waves but with weaker amplitudes (Fig. 4a). The S-waves, also reflected from the free surface, create yet another set of down-going reflected S- and converted P-waves. As shown in the snapshots the wave-field is fairly complex.

For Source 1, north of the basin, the sediment thickness increases southwards (Fig. 4b). Waves are reflected initially from the rock-alluvium interface and then the free surface. Waves affecting the north end of the basin will reach the free surface and be reflected before waves reach parts of the basin further south. The basin waves are multiply reflected from the top and bottom of the basin setting up what appears to be transient standing wave with increasing amplitudes. A coherent pattern of upward and downward traveling waves is created within the basin, that leads to ground roll (Rayleigh waves). Furthermore, there is scattering

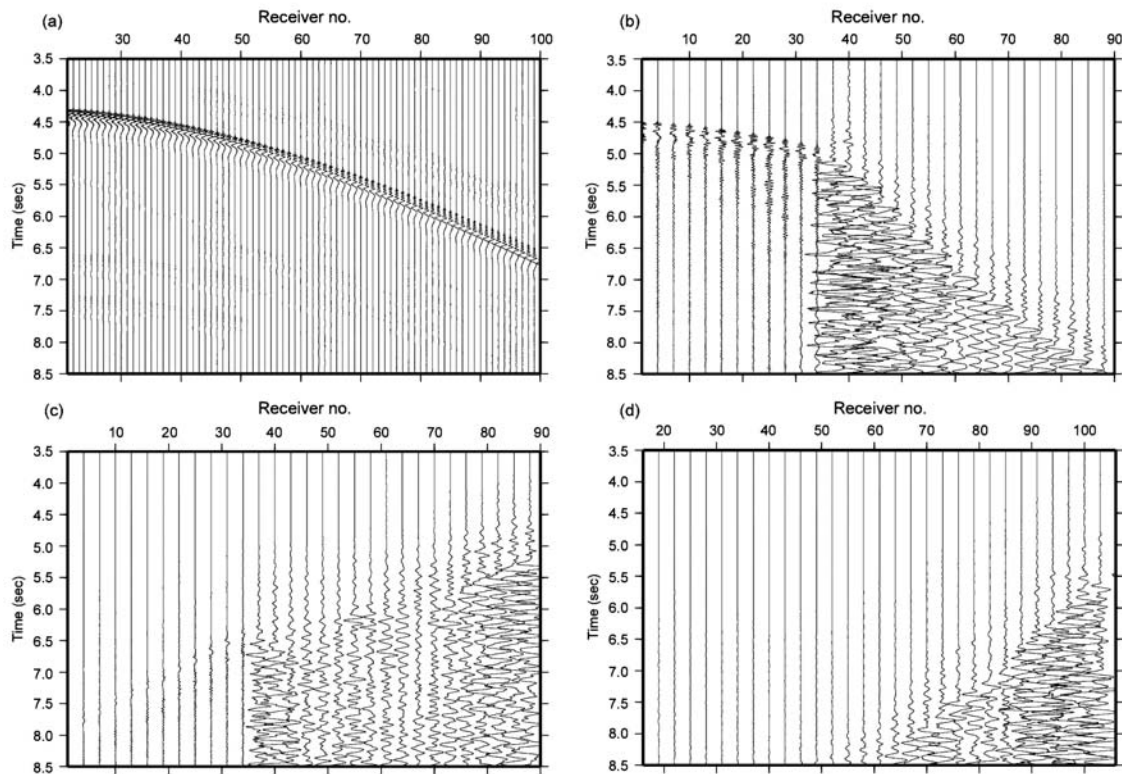


Figure 5. Seismograms corresponding to (a) model A with source 1; and model D with (b) source 1, (c) source 2, and (d) source 3.

(diffraction) from the northern margin of the basin where S- and P-waves leak into the crystalline crust. The basin vibrations continue even after the passage of the main S- and S-to-P waves, but naturally diminish with time.

For Source 2, south of the basin, the waves reach the thickest part of the basin first (Fig. 4c). Waves arriving later to the north will reach the surface before those that arrive earlier at the thicker parts of the basin. Thus, the pattern of wave interferences in the basin is different than for Source 1. The pattern of standing waves is irregular and the number of nodes is reduced to two. The waves lose energy in the thicker part of the basin and emerge weaker at the northern end.

For Source 3, from the east (Fig. 4d) the scenario is a combination of the two former cases. The basin is 'fixed' at both ends. A more coherent pattern of standing waves is established at the east end of the basin where the alluvium thickness is increasing away from the source. In the centre of the basin where depths are not changing much, wave incidence angles become nearly vertical. The thinning of the sediments at the western end creates a similar pattern to that for Source 2. Amplitudes remain high across most of the basin,

notwithstanding scattering from the basin bottom and the eastern hill-basin margin.

Figure 5 shows the seismograms corresponding to the snapshots of Figure 4. The seismograms for the control model show no amplification (Fig. 5a). To demonstrate the extent of wave-field amplifications within the basin, individual seismograms were taken from the receivers at the edges and centre of the basin and filtered sequentially between 1 and 10 Hz. A set of narrow bandpass filters with relative bandwidth of 0.5 Hz was used. In this analysis the amplitudes of the filtered traces for a specific source were compared to those on crystalline rock (Fig. 6). For the north-south transect, the traces used were, NS38, NS50, NS65 and NS85 (for positions see Fig 3a). NS38 is located at Constant Spring, which is at the margin of the basin at an elevation of 150 m with 60 m of sediments. NS50 is located where the basin deepens near Mary Brown's Corner, at an elevation of 130 m with an equivalent depth of alluvium. NS65 at Half-Way-Tree has an elevation of 80 m and overlies 500 m of alluvium, whereas NS85 in Downtown Kingston is at an elevation of 20 m overlying more than 600 m of sediments. The analysis revealed that the S-wave amplitudes

Enhanced earthquake risk of Kingston

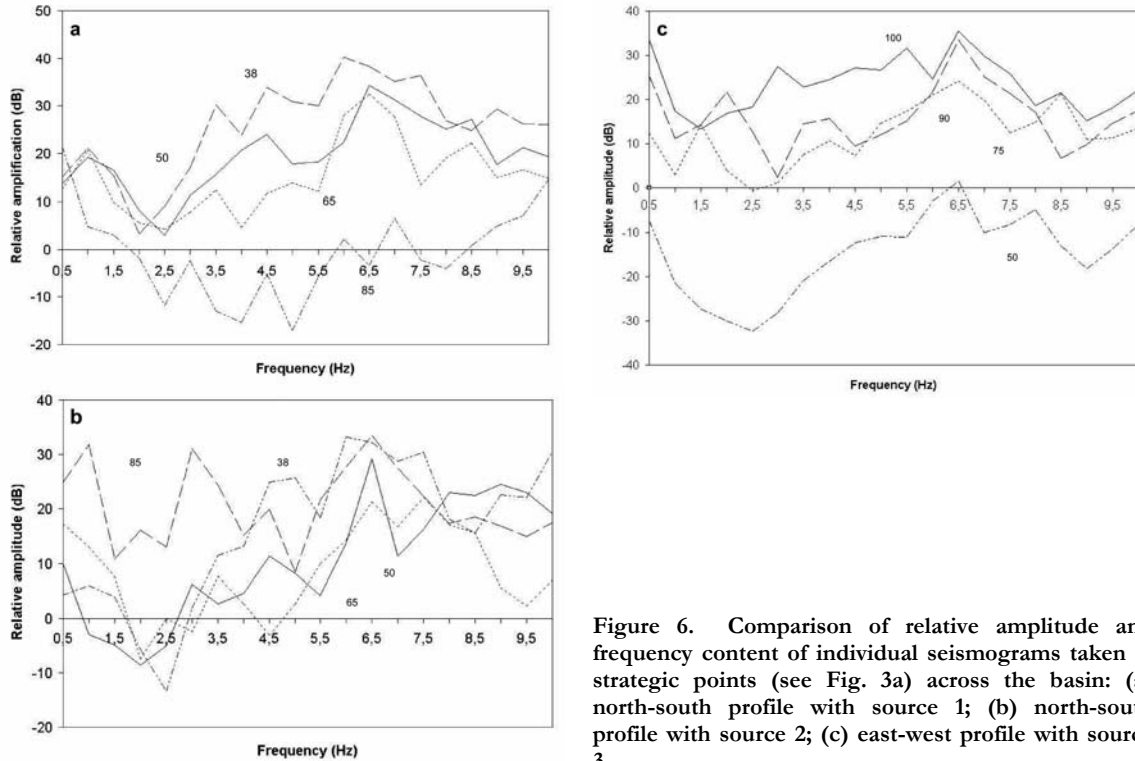


Figure 6. Comparison of relative amplitude and frequency content of individual seismograms taken at strategic points (see Fig. 3a) across the basin: (a) north-south profile with source 1; (b) north-south profile with source 2; (c) east-west profile with source 3.

increase by a factor of 5 in the central part of the basin and are largest at the margins by a factor of 10 (Fig. 6). For Source 1, (Fig. 5b) the amplitudes are increased by a factor of 10 at the northern basin-edge and then decrease gradually towards the centre of the basin to a factor of 5 relative to the rock. The seismograms for Source 2 (Fig. 5c) show highest amplitudes near the waterfront by a factor of 10. Similarly to source 1, the amplitudes decrease gradually towards the centre of the basin to a factor of 5. For the eastern source, (Fig. 5d) the highest amplitudes (factor of 10) are at the eastern end and these decrease progressively toward the centre of the basin (factor of 3). However, the amplitudes increase again at the western basin-edge by a factor of 6.

With regard to frequency content, for Source 1 at NS38, (Fig. 6a) all frequencies in the range 3-10 Hz are amplified, having peak amplitudes at 6 Hz. For NS50, while all frequencies are less amplified, there is a band of maxima around 6 Hz. For NS65, the peak amplitude at 6 Hz becomes more prominent. For Source 2, (Fig. 6b) the NS85 amplifications occurred for all frequencies with distinct peaks at 1, 3 and 6.5 Hz. Amplitudes at NS50 and NS65 were lower than at NS85. Again, there were maxima for all these receivers at around 6 Hz.

For the east-west profile (Fig 3-D), the seismograms at WE50 (alluvium thickness 400 - 500 m), WE75 (thickness ~ 400 m), WE90

(thickness ~ 170 m) and WE100 (thickness ~ 50 m) (for positions see Fig. 3a) were selected for evaluation of frequency content and relative amplitude amplification. On the west side, WE50 (Fig. 6c) showed insignificant amplification, with a very small maximum at 6.5 Hz. Near the centre of the basin, WE75 had a broad spectrum of prominent amplifications in the band 5 - 9 Hz. Nearer to the source, at WE90 two peaks emerged at 1-2 Hz and 5.5-8 Hz. At WE100, near to the basin-hill margin, all frequencies are amplified.

6. DISCUSSION

Waveform modelling is perhaps the best way to account for source and position variability in sedimentary basin ground motions (Field *et al.*, 2000). Furthermore, it has been shown that basin response is a greater factor in ground motion amplification than site response (Field *et al.*, 2000; Kebeasy and Husebye, 2003). It would have been optimal to be able to perform a 3-D synthesis of the response of the Liguanea Basin but the 3-D shape is not well known. However, 2-D synthetics have been shown to be representative of main wave-field features for simplified 2-D layered media (Hestholm and Ruud, 2000) like the Liguanea Basin.

Sources close to the Liguanea Plain were chosen, as there is ample evidence to suggest that

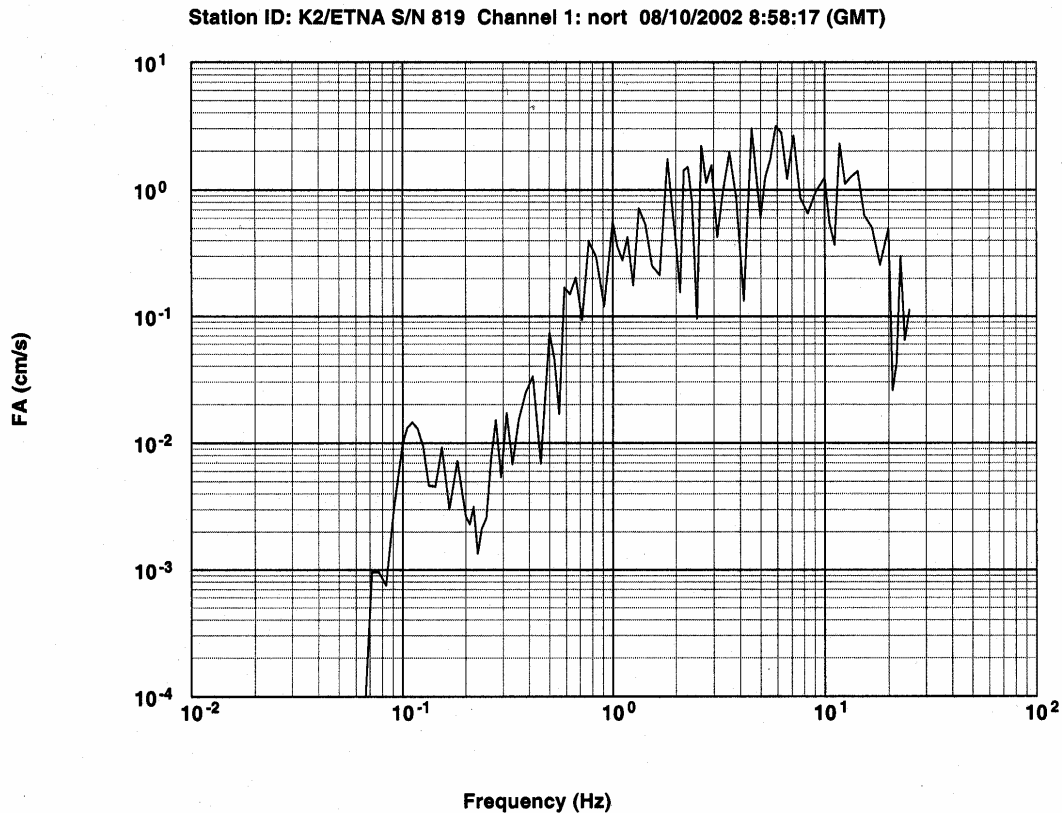


Figure 7. Fourier acceleration spectra recorded at Mona (near WE 100, Fig. 4a) for an earthquake on August 10, 2002, M4.6 that was widely felt on the Liguanea Plain (Intensity V) and other areas.

local earthquakes have played the dominant role in the occurrence of earthquake damage on the plain. Of the three source positions investigated in this study all are within 10 km of the basin and two, the north and east, are close to the basin-hill margins. The highest amplifications, by a factor of 10, were found at these margins, when compared to that for rock exposed at the surface outside of the basin. At the end furthest away from the source, particularly where sediment thickness exceeded 500 metres, the amplification was lower. At the centre of the basin, ground motion levels were lower by a factor of 2 than at the basin edges. This observation is in line with the basin-edge effect used to explain the damage patterns for the 1994 Northridge (Field *et al.*, 2000; Graves *et al.*, 1998) and 1995 Kobe (Kawase, 1996) earthquakes. The Liguanea Basin is a much smaller entity than the Los Angeles Basin with maximum depths of 0.7 and 10 km, respectively. As was noted earlier, the high impedance contrast between the rock layers and the overlying alluvium could account for more energy being reflected than transmitted at the basin bottom. In addition, in the thick Los Angeles Basin, an

increased wave energy absorption takes place within the basin, but as demonstrated above, such effects are of marginal importance for the Liguanea Basin.

The 2-D simulation confirms that the levels of amplification across the basin vary significantly. Seismic hazard assessments typically determine levels of amplification on rock and do not adequately incorporate 2-D changes in amplification taking place over small distances, like across the Liguanea Basin.

Synthetic wave-field results compare largely with the intensity pattern for the 1993 earthquake (Fig. 2) giving lower amplification in the basin centre, near Half-Way-Tree (HWT), where intensities of V and even IV were reported. The neighboring New Kingston area, which is just east of the NS transect, showed consistently higher intensities by a factor of 1 to 2 units. In general, higher intensities of VII were seen around the edges of the basin, including the waterfront area, where a few buildings of medium height had damaged columns (Adams, 1996). In basin-hill margins like August Town and Barbican (just north of Liguanea), single storey dwellings were affected by

Enhanced earthquake risk of Kingston

minor to severe cracking of walls, though poor construction and back-filled gully courses being used for development, were seen as parts of the problems in those areas, respectively (Harris, 1996). Barbican and August Town, however, are not only situated at the edge of the basin, but at the edge closest to the north-east source of the 1993 earthquake. The results of this study show that amplitudes of ground motion could have been 10 or more times higher in these basin-edge zones than on rock and 5 times higher than in the basin centre. The waterfront has the additional problem of a high water table and is prone to liquefaction from historical accounts. These non-linear factors were not accommodated in the model. The intensity map corroborates at least the idea of the variability of intensities across the Liguanea Plain, within a factor of 2 intensity units and points to the additional problem of the Mona sub-basin, which is situated east of Long Mountain, and has not been addressed in this 2-D study.

The frequency of 6 to 6.5 Hz (or 0.16 to 0.15 sec. period) appears to be representative of the natural frequency for the Liguanea alluvium. The results show that a wide spectrum of frequencies was amplified at the edges of the basin and this narrowed near the centre, with 6 Hz becoming dominant. Based on the approximate formula of 0.1 sec. per storey for the natural period of buildings, these results suggest that high-frequency low-rise buildings are at a higher risk on deeper sediments near the middle of the fan, for near earthquake sources. Buildings of all frequencies between 1 and 10 Hz appear to be at increased risk near the basin edges. At the deep end of the basin, at Kingston waterfront and in the city centre or downtown area, the excited frequencies shift towards 10 Hz, and the levels of amplification become lower when spreading is increased. However, the limitation that beyond the ends of both transects, the basin shape is still unknown must be remembered in discussing basin edge effects, especially at the southern and western ends of the models. It is interesting to note that a strong motion recording made at Mona, for a recent felt earthquake (Md 4.6, August 10, 2002) off the east coast of Jamaica, revealed peak amplitudes of 2 cm/s at frequencies around 6 Hz which coincides well with the results of this study (Fig. 7).

7. CONCLUSIONS

This 2-D synthesis has been instructive in showing that wave-field excitation in the Liguanea Basin from local earthquake sources is significant. Moreover, the amplification is variable across the

basin, dependant on source position and location within the basin. This lateral response needs to be included to reflect the full extent of earthquake risk in Kingston, Jamaica. The Liguanea Basin sediments preferentially amplify frequencies at and around 6 Hz, or the equivalent natural period of 0.167 sec. Basin-edges though, amplify over a broader spectrum of frequencies. The basin margins where sediments are often thinner and meet the positive topography have amplifications consistently (a factor of 10) larger than found in the centre (a factor of 5), irrespective of source position. Low Q in the uppermost crystalline crust and the basin sediments only marginally reduces the wave-field amplitudes, as expected.

Acknowledgements. *The authors sincerely thank the following persons and institutions without whom this study would not have been possible: Stig Hestholm and Bent-Ole Ruud for allowing us to use their Finite Difference software; Bent-Ole Ruud for help with interpreting the synthetics and reviewing the manuscript; Yuri Fedorenko for assistance with generating some of the figures, and reviewing the manuscript; the Research Council of Norway (Program for Supercomputing) for allowing us time on the supercomputer in Trondheim; and the Government of Norway for financial support.*

REFERENCES

- Adams, A. 1996.** A review of the effects of the January 13, 1993 earthquake and building code provisions. *Journal of the Geological Society of Jamaica*, **30**, 41-48.
- Ahmad, R. and Robinson, E. 1994.** Geological evolution of the Liguanea Plain – the landslide connection. In **Greenfield M. and Robinson R. (Eds).** *Proceedings of the First Conference, Faculty of Natural Sciences; The University of the West Indies, Mona*, 22-23.
- De Mets, C., Jansma, P.E., Mattioli, G.S., Dixon, T., Farina, F., Bilham, R., Calais, E., and Mann, P. 2000.** GPS Geodetic constraints on Caribbean-North America Plate Motion. *Geophysical Research Letters*, **27**, 437-440.
- Field, E.H. and the SCEC Phase III Working Group 2000.** Accounting for Site Effects in Probabilistic Seismic Hazard Analyses of Southern California: Overview of the SCEC Phase III Report. *Bulletin of the Seismological Society of America*, **90**, S1-31
- Graves, R.W, Pitarka, A. and Somerville, P.G. 1998.** Ground-Motion Amplification in the Santa Monica Area: Effects of Shallow Basin-Edge Structure. *Bulletin of the Seismological Society of America*, **88**, 1224-1242
- Harris, N. 1996.** Preliminary Observations of Ground Response and Performance of Non-Engineered Buildings: The January 13, 1993 Earthquake. *Journal of the Geological Society of Jamaica*, **30**, 32-40.

- Hestholm, S.O. and Ruud, B. O. 2000.** 2-D finite-difference viscoelastic wave modeling including surface topography. *Geophysical Prospecting*, **48**, 341-373.
- Jamaica Seismograph Network Bulletin 1992 & 1993.** *Earthquake Unit, University of the West Indies, Mona 2000*, **5**, 126 pp.
- Kagawa, 1995.** *Shake 21 for the Windows operating system*, Geotechnical Research Group, Department of Civil Engineering, Wayne State University, Detroit Michigan, 23 pp.
- Kawase, H. 1996.** The cause of the Damage Belt in Kobe: "The Basin-Edge Effect," Constructive Interference of the Direct S-Wave with the Basin-Induced Diffracted/Rayleigh Waves. *Seismological Research Letters*, **67**, 25-34.
- Kebeasy, T. and Husebye, E.S., 2003.** A finite-difference approach for simulating ground responses in sedimentary basins: qualitative modelling of the Nile Valley, Egypt. *Geophysical Journal International*, **154**, 1-12.
- Mendi, C.D., Ruud, B.O. and Husebye, E.S. 1997.** The North Sea Lg-blockage puzzle. *Geophysical Journal International*, **130**, 669-680.
- National Disaster Research, Inc.; The Earthquake Unit, UWI; Mines and Geology Division, Jamaica; 1999.** *Kingston Metropolitan Area Seismic Hazard Assessment Final Report*. Prepared for the U.S. Agency for International Development/Organization of American States, Caribbean Disaster Mitigation Project, Kingston Multi-Hazard Assessment: 82 pp.
- Perrot, J., Calais, E., Mercier de Lepinay, B. 1997.** Waveform simulation of the May 25th, 1992, Ms 6.7 Cabo Cruz earthquake (Cuba): NWE constraints on the tectonic regime along the Northern Caribbean Plate Boundary. *Pure and Applied Geophysics*, **149**, 475-487.
- Ruud, B.O. and Hestholm, S. 2001.** 2-D surface topography boundary conditions in seismic wave modeling. *Geophysical Prospecting*, **49**, 445-460.
- Shepherd, J.B. and Aspinall, W.P. 1980.** Seismicity and seismic intensities in Jamaica, West Indies: A problem in risk assessment. *Earthquake Engineering and Structural Dynamics*, **8**, 315-335.
- Tomblin, J.M. and Robson, G.R. 1977.** A catalogue of felt earthquakes for Jamaica with reference to other islands in the Greater Antilles. Jamaica Ministry of Mining and Natural Resources, *Mines and Geology Division Special Publication No. 2*, 243 pp.
- Van Dusen, S.R., Doser, D.I. 2000.** Faulting process of historic (1917–1962) M = 6.0 Earthquakes along the north-central Caribbean margin. *Pure and Applied Geophysics*, **157**, 719-736.
- Wiggins-Grandison, M.D. 1996.** Seismology of the January 1993 earthquake. *Journal of the Geological Society of Jamaica*, **30**, 1-14.
- Wiggins-Grandison, M.D. 2001.** Preliminary results from the new Jamaica Seismograph Network. *Seismological Research Letters*, **72**, 525-537.

Revised version received: February 22nd 2003
 Accepted: February 28th 2003